The connection between disk accretion and stellar mass

James Muzerolle[1,2], Nuria Calvet[3], Lee Hartmann[3], César Briceño[2,4], Lynne Hillenbrand[2,5], and Jesús Hernández[4,6]

ABSTRACT

We present evidence for a correlation between disk mass accretion rates and masses in 1-3 Myr-old pre-main sequence objects ranging from brown dwarfs to progenitors of Herbig Ae stars. Using observations and models of Hα emission lines and UV/optical continuum excesses in very low mass objects and intermediate mass T Tauri stars, we have calculated mass accretion rates over an unprecedented range of masses. In combination with existing measurements at $\sim 0.5\ M_\odot$, we find that the mean mass accretion rate changes from $\sim 10^{-11} - 10^{-6}\ M_\odot\, yr^{-1}$ for masses ranging from $0.04-4\ M_\odot$, with an overall proportionality of $\dot{M} \propto M_*^{2.3}$. The upper envelope of this correlation is in agreement with upper limits expected for non-self-gravitating disks (where $M_d \lesssim 0.1 M_*$). However, the physical origin of the general $\dot{M}$ versus M_* trend is not clear, since standard viscous accretion disk models do not predict as steep a correlation as we find here. We suggest that X-ray ionization of the disk may provide a mass-dependent source of angular momentum transport; this possibility should be explored by further theoretical work.

Subject headings: accretion disks, brown dwarfs, stars: emission-line, pre-main sequence, circumstellar matter,

---

[1]Steward Observatory, 933 N. Cherry Ave., University of Arizona, Tucson, AZ 85721

[2]Visiting Astronomer, W. M. Keck Observatory, which is operated as a scientific partnership among the California Institute of Technology, the University of California, and the National Aeronautics and Space Administration. The Observatory was made possible by the generous financial support of the W. M. Keck Foundation.

[3]Smithsonian Astrophysical Observatory, 60 Garden St., Cambridge, MA 02138

[4]Centro de Investigaciones de Astronomia (CIDA), Apartado Postal 264, Mérida 5010-A, Venezuela

[5]Dept. of Astronomy, MS105-24, California Institute of Technology, Pasadena, CA 91125

[6]Postgrado de Física Fundamental, Universidad de Los Andes (ULA), Mérida 5101-A, Venezuela

1. Introduction

The rate of accretion through pre-main sequence circumstellar disks has important implications for star and planet formation, because most of a typical star's mass is probably accreted through its disk, and planet formation and migration can be sensitive to the details of the accretion process (e.g., Hartmann 1998; Lin et al. 2000; Ward & Hahn 2000). Understanding how accretion rates vary as a function of age and other parameters can provide important clues to the physical mechanism(s) underlying the accretion process, and thus improve our understanding of the formation of stars and associated planetary bodies.

The stellar mass is likely to be an important parameter in disk accretion. If stars are formed from disks, the mass accretion rates might need to be higher – at least in very early stages – for higher mass stars, to form them rapidly enough. Accretion rates might also depend upon the disk mass, which in turn could depend on the stellar mass; disks more massive than about 0.1-0.2 times the stellar mass are thought to be rare, as they tend to be gravitationally unstable and likely to accrete rapidly (e.g., Pringle 1981).

To date, measured accretion rates for pre-main sequence stars have been dominated by studies of objects over a relatively small mass range. Here, we examine recent measurements of accretion rates for young objects spanning two orders of magnitude in mass, including brown dwarfs and intermediate mass T Tauri stars, in order to study the mass dependence of accretion rates. Our findings suggest a strong correlation with (sub)stellar mass, which may be difficult to reconcile with some theories of pre-main sequence disk accretion.

2. Measurement of mass accretion rates

The presently accepted paradigm for mass loading from the disk onto the star for the well-studied ($M_* \sim 0.3 - 0.8 M_\odot$) Classical T Tauri stars (CTTS) is the magnetospheric accretion model (Uchida & Shibata 1985; Bertout, Basri, & Bouvier 1989; Königl 1991; Calvet & Hartmann 1992; Shu et al. 1994). In brief, the inner disk of CTTS is truncated by the stellar magnetic field, and matter falls onto the star along magnetic field lines. Broad emission lines are formed in this free-falling flow (Muzerolle et al. 1998, 1999, 2001 = MCH). Material merges into the photosphere through an accretion shock, which is responsible for the excess emission that veils the absorption lines in the optical and dominates in the ultraviolet (Calvet & Gullbring 1998; Gullbring et al. 2001). We have now provided convincing evidence that the magnetospheric accretion model applies over a factor of 100 in mass, $0.04 M_\odot \le M_* \le 4 M_\odot$, based on observations and models of both broad, permitted emission lines such as Hα (Muzerolle et al. 2000a; Muzerolle et al. 2003, hereafter, MHCBH) and UV continuum excesses (Calvet et al. 2003, CMBHHS, in preparation). We next review the determination of mass accretion rates from these analyses.

Mass accretion rates at the substellar limit. We obtained spectra for a sample of 45 known very low mass (VLM) objects with spectral types M4-M8.5, located in several different star forming regions and young clusters, including Taurus, IC 348, σ Ori, Upper Sco, and ρ Oph. The masses of the VLM objects span the substellar boundary, ranging from 0.04-0.23 $M_\odot$. Details of the observations and interpretation were reported in MHCBH. We identified a total of 13 accretors in the VLM sample, using the most sensitive signpost of magnetospheric accretion, namely broad (>200 km s^{-1}) and asymmetric Hα emission profiles, as well as other diagnostics such as forbidden line emission or Ca II triplet emission equivalent widths stronger than typical dwarf/weak T Tauri star levels. The accretors are listed in Table 1, together with their spectral type, luminosity, and mass, taken from MHCBH.

We calculated Hα profiles for the lowest mass objects in the accretor sample using the radiative transfer models of Balmer emission line profiles previously applied to the $\sim 0.5\ M_\odot$ CTTS (MCH). Matching these models to the observed profiles, we derived mass accretion rates for the VLM sample, also listed in Table 1. For the higher mass objects in the sample, we estimated accretion rates from veiling measurements (see MHCBH).

Mass accretion rates for intermediate mass TTS. We obtained ultraviolet spectra with STIS/MAMA on the *Hubble Space Telescope* (HST) for a sample of 9 intermediate mass T Tauri stars (IMTTS), located in Taurus-Auriga, the outer regions of the Orion Nebula Cluster, and the ring around λ Ori. To complement the HST observations, we obtained simultaneous UBVRI photometry, as well as optical spectra, which allowed us to obtain consistent spectral types. Details of the observations and data reduction are given in CMBHHS.

Accretion shock models, calculated according to the procedures of Calvet & Gullbring (1998), were applied to the ultraviolet and optical spectro-photometric observations, allowing us to estimate accretion luminosities for the IMTTS sample. Table 2 shows the mass accretion rates derived from the accretion luminosity estimates, given the listed stellar masses and radii. The main uncertainties in the determination of $\dot{M}$ arise from uncertainties in the reddening law, as well as the spectral type. We estimate these uncertainties to be roughly a factor of 3 (see discussion in CMBHHS).

3. The mass accretion rate vs. mass correlation

The mass accretion rates are plotted against stellar mass in Figure 1. We show here the samples of VLM objects and IMTTS discussed in this work, as well as all the other CTTS in Taurus for which mass accretion rates have been determined in previous investigations, including binary components (see references in the figure caption). A remarkable trend of increasing $\dot{M}$ with M_* is apparent, spanning ~ 5 orders of magnitude in mass accretion rate and ~ 2 orders of magnitude in mass. This mass range encompasses brown dwarfs, T Tauri stars, and progenitors of Herbig Ae stars. A correlation between $\dot{M}$ and M_* has been reported before for the low mass end (White and Basri 2003; MHCBH), but we show here that the correlation holds over a much larger range of masses. The approximate proportionality of the correlation is $\dot{M} \propto M_*^{2.3}$.

Several caveats must be considered when interpreting the $\dot{M}$ vs. M_* correlation. One is that the masses and mass accretion rates are dependent on the evolutionary tracks used. Masses and accretion rates for the objects shown in Figure 1 have been calculated using the Siess, Dufour, & Forestini (2000) tracks for the IMTTS and CTTS, and the Baraffe et al. (1998) tracks for the VLM objects. Both sets of tracks are similar in the region where they overlap, and are consistent with empirical mass determinations (e.g., Simon, Dutrey, & Guilloteau 2000). When mass accretion rates are derived from accretion luminosities, as in the case of the CTTS and IMTTS, the $\dot{M}$ values change in inverse proportion to the mass, since $L_{acc} \sim GM_*\dot{M}/R_*$. On the other hand, an increase in stellar mass would result in higher magnetospheric infall velocities, which in turn result in smaller magnetospheric gas densities; to obtain the same fluxes, $\dot{M}$ should be increased. Thus, when mass accretion rates are derived from line profile modeling, $\dot{M}$ would change approximately as the square root of a change in mass (see MCH). This would tend to flatten the slope of the correlation, although any change would be fairly small. For instance, if the D'Antona & Mazzitelli (1997) tracks are used instead of Siess et al. (2000), then the best-fit slope of the $\dot{M}$ vs. M_* correlation would be 2.1. Therefore, this effect is much smaller than any spread due to intrinsic variability and other uncertainties in the $\dot{M}$ determination.

Another question to be raised is whether the observed correlation is a result of selection bias – objects accreting at low levels may be missed because of limitations of the methods of detection. We determined minimum mass accretion rates for producing observable broad Hα emission profiles, the most sensitive accretion diagnostics, from the magnetospheric accretion models (see discussion in MHCBH). Figure 1 shows these minimum values for three different stellar masses. For the CTTS (~ 0.5 $M_\odot$), the predicted minimum $\dot{M}$ is more than an order of magnitude lower than the lowest measured value at that mass, indicating that the observed lower limit to $\dot{M}$ is probably real. On the other hand, the lowest $\dot{M}$ values for the VLM sample are closer to the minimum detection limit, so the completeness there is somewhat more ambiguous. The situation is less clear regarding the IMTTS. In contrast to the CTTS and VLM objects, the sample of IMTTS is small, and was selected on the basis of Hα emission, which must dominate over the photospheric absorption in order to be readily detected in low-resolution spectra of these hotter, higher mass objects. Our Hα models indicate that the accretion rate cannot be lower than about $10^{-8}\ M_{\odot}\,yr^{-1}$ for this to be the case. In addition, the relatively bluer photospheres of these stars would preclude measuring UV excesses, and hence accretion rates, if $\dot{M} \lesssim 10^{-8} M_{\odot}\,yr^{-1}$. Thus, there may be a bias towards higher accretion rates in the IMTTS sample. Larger samples of IMTTS need to be analyzed in order to confirm our observed $\dot{M}$ lower limit. We note that our Hα models do predict the presence of redshifted absorption, with no emission component, for $\dot{M} \sim 10^{-9}\ M_{\odot}\,yr^{-1}$ in IMTTS; observations of residual profiles, with the photospheric absorption component subtracted off, may reveal such features if IMTTS with low accretion rates in fact exist.

Finally, we comment on stellar ages. The CTTS and VLM samples shown in Figure 1 have similar ages, 1-3 Myr (Hartmann 2003; MHCBH), while the IMTTS range in age from 1 - 8 Myr (CMBHHS). However, it is a well-known effect that IMTTS tend to appear older than the low mass and high mass stars of a given cluster or association (Hillenbrand 1997), which may be due to birthline effects (Hartmann 2003). In any event, the low mass populations of the associations to which our IMTTS sample belong also have ages $\sim$ 1 - 3 Myr (Hartmann 2003; Hillenbrand 1997; Dolan & Mathieu 2002). Thus, systematic effects due to age, where older objects are expected to have lower accretion rates on average due to disk evolution (e.g., Muzerolle et al. 2000b), should not be present in the results shown here.

4. Discussion

We can predict the upper envelope of the mass-$\dot{M}$ correlation by assuming that disk masses must be near or below the limit for gravitational stability in order to last for any significant length of time. Taking a crude disk mass limit of $\sim 0.1 M_*$, and adopting a typical age of $\sim$ 1 Myr for our program objects, we then expect to find few if any objects accreting faster than $\dot{M} \approx 10^{-7}\ (M_*/M_{\odot})\ M_{\odot}\,yr^{-1}$. Figure 1 shows that this limit is generally satisfied, with the exception of just a few objects; the agreement is excellent given the uncertainties in the $\dot{M}$ measurements and ages, and the probability of time variable accretion rates for individual objects.

The trend of accretion rates shown in Figure 1 appears to be steeper than $\dot{M} \propto M_*$.

However, this cannot be taken as a firm result before we better understand the selection effects among the higher-mass stars in the sample. These stars in particular were selected for strong Hα emission (and thus probably for high accretion), as discussed in §3. In addition, it is difficult to detect low accretion rates in hotter stars. However, the absence of objects above the mass limit is robust.

Hartmann et al. (1998) considered simple viscous disk similarity solutions for young stars. These models exhibit a disk accretion rate which at any time is roughly

$$\dot{M} \approx M_d/t_\nu \,, \tag{1}$$

where M_d is the disk mass, and t_ν is a characteristic viscous time evaluated, for example, at the disk half mass radius $R_{1/2}$. Qualitatively, this model predicts that for a given stellar mass, the disk accretion rate should decrease with increasing age, because the disk expands and the viscous time becomes longer.

In an α-disk model (Shakura & Sunyaev 1973; Pringle 1981), the viscous time scales as

$$t_\nu(R_{1/2}) \propto (R_{1/2}^2 \Omega/(\alpha T_{1/2}) \propto M_*^{1/2}\, R_{1/2}^{1/2}\, (\alpha T_{1/2})^{-1} \,. \tag{2}$$

Here we have assumed that the disk rotation is keplerian with angular frequency Ω. If we make the assumption that disk heating is dominated by irradiation from the central star (Kenyon & Hartmann 1987; D'Alessio etal 1998), then we expect, roughly, $T_{1/2} \propto L_*^{1/4} R_{1/2}^{-1/2}$, where L_* is the stellar luminosity. Taking the initial disk mass to be at the limit for gravitational stability,

$$\dot{M} \propto \alpha\, M_*^{1/2}\, R_{1/2}^{-1}\, L_*^{1/4} \,. \tag{3}$$

For example, if average disk radii were similar, and α were constant, then $\dot{M} \propto M_*^{1/2} L_*^{1/4}$. The luminosities of our objects vary by about 4 orders of magnitude over 2 orders of magnitude in mass, or $L_* \approx M_*^2$, so this would yield $\dot{M} \propto M_*$. This illustrates some dependence of $\dot{M}$ on mass, although weaker than implied by Figure 1.

In any case, the validity of simple constant-α models is seriously in question for pre-main sequence disks. It has been shown that the magnetorotational instability (MRI) can be extremely effective in producing angular momentum transport in astrophysical disks (e.g., Balbus & Hawley 1998), and can be treated in an α prescription (Balbus & Papaloizou 1999). However, standard models of protostellar/protoplanetary disks indicate that ionization levels are too low for the MRI to operate over substantial regions in the such disks (Gammie 1996; Sano et al. 2000; but see Fromang, Terquem, & Balbus 2002 for a somewhat more optimistic view). In the theory of Gammie (1996), accretion of non-self-gravitating disks only occurs in "active" upper disk layers with sufficiently high ionization (outside of the innermost disk regions, where thermal ionization can be sufficient). Originally, Gammie supposed that cosmic rays ionized the disk to roughly a constant surface density; this limits the mass accretion rate (proportional to the active surface density) to a constant value. As pointed out by Armitage, Livio, & Pringle (2001), such constant accretion rates do not seem to agree with the evidence for a decay in mass accretion rates with increasing age. In our case, the cosmic-ray-driven active layer model also has problems because there is no scaling of accretion rate with stellar mass. There are also concerns on whether cosmic rays can effectively penetrate the disk, or whether they are scattered by pre-main sequence disk winds.

Stellar X-rays have been suggested as an alternative ionization source for disk active layers (Glassgold, Najita, & Igea 1997; Igea & Glassgold 1999). Recent observations of X-rays from young stellar objects indicate that the X-ray luminosity L_X scales approximately as the stellar mass squared (e.g. Flaccomio et al. 2002; Feigelson et al. 2002). One might then expect an increase in ionization, and thus in disk accretion rate, with increasing mass over our range. However, it is far from clear that this can account for the steep trend we observe. The column density of the active layer is limited at very low levels of ionization, where the X-ray penetration is being exponentially attenuated; thus the variation of active layer column density, and therefore of mass accretion rates, should be very much smaller than the change in L_X. Calculations of disk ionization which explicitly vary L_X should be made to investigate this problem further.

In summary, our results indicate a strong trend of increasing mass accretion rate as a function of increasing stellar mass for pre-main sequence objects. This correlation offers an important challenge for theories of disk accretion.

Part of this work was supported by NASA through grant GO-08317.01-97A from the Space Telescope Science Institute and Origins of Solar Systems grant NAG5-9670 to NC and LH.

REFERENCES

Armitage, P. J., Livio, M., & Pringle, J. E. 2001, MNRAS, 324, 705

Balbus, S. A. & Hawley, J. F. 1998, Reviews of Modern Physics, 70, 1

Balbus, S. A. & Papaloizou, J. C. B. 1999, ApJ, 521, 650

Baraffe, I., Chabrier, G., Allard, F., & Hauschildt, P. H. 1998, A&A, 337, 403

Bertout, C., Basri, G., & Bouvier, J. 1988, ApJ, 330, 350

Calvet, N. & Gullbring, E. 1998, ApJ, 509, 802

Calvet, N. & Hartmann, L. 1992, ApJ, 386, 239

Chabrier, G., Baraffe, I., Allard, F., & Hauschildt, P. 2000, ApJ, 542, 464

D'Alessio, P., Cantó, J., Calvet, N., & Lizano, S. 1998, ApJ, 500, 411

D'Antona, F. & Mazzitelli, I. 1997, Mem. Soc. Astron. Italiana, 68, 807

Dolan, C. J. & Mathieu, R. D. 2002, AJ, 123, 387

Flaccomio, E., Damiani, F., Micela, G., Sciortino, S., Harnden Jr., F. R., Murray, S. S., & Wolk, S. J. 2003, ApJ, 582, 398

Feigelson, E. D., Gaffney III, J. A., Garmire, G., Hillenbrand, L. A., & Townsley, L. 2003, ApJ, 584, 911

Fromang, S., Terquem, C., & Balbus, S. A. 2002, MNRAS, 329, 18

Gammie, C. F. 1996, ApJ, 457, 355

Glassgold, A. E., Najita, J., & Igea, J. 1997, ApJ, 480, 344

Gullbring, E., Calvet, N., Muzerolle, J., & Hartmann, L. 2000, ApJ, 544, 927

Hartmann, L. 1998, Accretion processes in star formation / Lee Hartmann. Cambridge, UK; New York : Cambridge University Press, 1998. (Cambridge astrophysics series; 32)

Hartmann, L. 2003, ApJ, 585, 398

Hartmann, L., Calvet, N., Gullbring, E., & D'Alessio, P. 1998, ApJ, 495, 385

Hillenbrand, L. A. 1997, AJ, 113, 1733

Igea, J. & Glassgold, A. E. 1999, ApJ, 518, 848

Kenyon, S. J. & Hartmann, L. 1987, ApJ, 323, 714

Königl, A. 1991, 1991, ApJ, 370, L39

Lin, D. N. C., Papaloizou, J. C. B., Terquem, C., Bryden, G., & Ida, S. 2000, Protostars and Planets IV, 1111

Muzerolle, J., Briceño, C., Calvet, N., Hartmann, L., Hillenbrand, L., & Gullbring, E. 2000a, ApJ, 545, L141

Muzerolle, J., Calvet, N., Briceño, C., Hartmann, L., & Hillenbrand, L. 2000b, ApJ, 535, L47

Muzerolle, J., Calvet, N., & Hartmann, L. 1998a, ApJ, 492, 743

Muzerolle, J., Calvet, N., & Hartmann, L. 2001a, ApJ, 550, 944 (MCH)

Muzerolle, J., Hillenbrand, L., Calvet, N., Briceño, C., & Hartmann, L. 2003, ApJ, in press (MHCBH)

Pringle, J. E. 1981, ARA&A, 19, 137

Sano, T., Miyama, S. M., Umebayashi, T., & Nakano, T. 2000, ApJ, 543, 486

Shakura, N. I & Sunyaev, R. A. 1973, A&A, 24, 337

Shu, F., Najita, J., Ostriker, E., Wilkin, F., Ruden, S., & Lizano, S. 1994, ApJ, 429, 781

Siess, L., Dufour, E., & Forestini, M. 2000, A&A, 358, 593

Simon, M., Dutrey, A., & Guilloteau, S. 2000, ApJ, 545, 1034

Uchida & Shibata 1985, PASJ, 37, 515

Ward, W. R. & Hahn, J. M. 2000, Protostars and Planets IV, 1135

White, R. J. & Basri, G. 2003, ApJ, 582, 1109

This preprint was prepared with the AAS LATEX macros v5.0.

Table 1. Properties of the very low mass young objects

object	SpT	log L_{bol} ($L_\odot$)	M_* ($M_\odot$)	log $\dot{M}$ ($M_\odot\, yr^{-1}$)
MHO-5	M6	-1.18	0.09	-10.8
MHO-6	M4.75	-1.16	0.13	-10.3
CIDA 14	M5	-0.64	0.12	-10.3
IC348-165	M5.25	-0.98	0.12	-10.0
IC348-173	M5.75	-0.95	0.10	-10.0
IC348-205	M6	-1.11	0.09	-10.0
IC348-336	M5.5	-1.40	0.10	-10.0
IC348-415	M6.25	-2.00	0.04	-9.3
IC348-382	M6.5	-1.91	0.04	-10.8
V410 Anon13	M5.75	-1.45	0.08	-11.3
Haro 6-28	M2.5	-0.82	0.23	-8.7
LkHα 358	K7-M0	0.88	0.23	-8.5
FP Tau	M2.5	-0.49	0.22	$<$-9

Note. — See MHCBH

Table 2. Properties of the Intermediate Mass T Tauri stars

object	SpT	log L_{bol} ($L_\odot$)	M_* ($M_\odot$)	log $\dot{M}$ ($M_\odot\, yr^{-1}$)
SU Aur	G2	1.15	2.0	-7.1
T Tau	K1	1.1	2.5	-6.8
RY Tau	G5	1.1	1.9	-6.8
EZ Ori	G0	1.03	1.7	-7.2
P2441	G0	1.1	1.8	-7.6
V1044 Ori	G5	0.9	1.7	-7.3
CO Ori	G0	1.6	2.7	-6.3
GW Ori	G5	2.0	4.0	-5.7
GX Ori	K1	0.6	1.7	-7.2

Note. — See CMBHHS

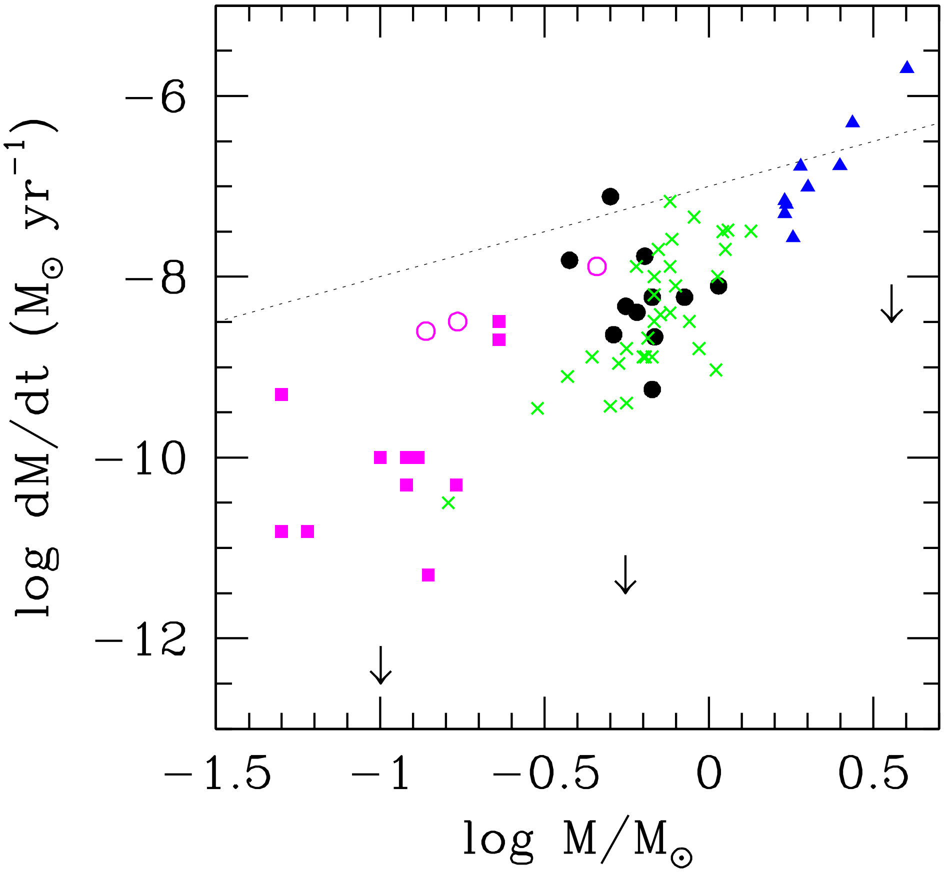

Fig. 1.— The relation between mass accretion rate and stellar mass. Squares represent $\dot{M}$ values measured by Muzerolle et al. (2000a) and MHCBH; solid circles are from Gullbring et al. (1998) (omitting binaries); crosses are from White & Ghez (2000) (including binary components); open circles are from White & Basri (2003); triangles are from CMBHHS. All the previously published values for the CTTS have been adjusted according to the masses derived from the Siess et al. (2000) tracks. The dashed line represents the maximum mass accretion rate allowed for gravitationally stable accretion disks (see text), while the arrows represent $\dot{M}$ lower limits for observable Hα emission predicted by magnetospheric accretion models.